THE JOURNAL OF BIOLOGICAL CHEMISTRY VOL. 286, NO. 39, pp. 34015–34022, September 30, 2011

Unique Ganglioside Recognition Strategies for Clostridial Neurotoxins*[S]

Received for publication, June 14, 2011, and in revised form, August 3, 2011 Published, JBC Papers in Press, August 17, 2011, DOI 10.1074/jbc.M111.272054

Marc A. Benson[‡], **Zhuji Fu**[§], **Jung-Ja P. Kim**[§], **and Michael R. Baldwin**[‡1]

From the [‡]*Department of Molecular Microbiology and Immunology, University of Missouri, Columbia, Missouri 65212 and the* [§]*Department of Biochemistry, Medical College of Wisconsin, Milwaukee, Wisconsin 53226*

Botulinum neurotoxins (BoNTs) and tetanus neurotoxin are the causative agents of the paralytic diseases botulism and tetanus, respectively. The potency of the clostridial neurotoxins (CNTs) relies primarily on their highly specific binding to nerve terminals and cleavage of SNARE proteins. Although individual CNTs utilize distinct proteins for entry, they share common ganglioside co-receptors. Here, we report the crystal structure of the BoNT/F receptor-binding domain in complex with the sugar moiety of ganglioside GD1a. GD1a binds in a shallow groove formed by the conserved peptide motif E . . . H . . . SXWY . . . G, with additional stabilizing interactions provided by two arginine residues. Comparative analysis of BoNT/F with other CNTs revealed several differences in the interactions of each toxin with ganglioside. Notably, exchange of BoNT/F His-1241 with the corresponding lysine residue of BoNT/E resulted in increased affinity for GD1a and conferred the ability to bind ganglioside GM1a. Conversely, BoNT/E was not able to bind GM1a, demonstrating a discrete mechanism of ganglioside recognition. These findings provide a structural basis for ganglioside binding among the CNTs and show that individual toxins utilize unique ganglioside recognition strategies.

The seven serotypes of botulinum neurotoxin (BoNT/A–G),[2] notorious as the causative agents of botulism, are extremely potent neuromuscular poisons (1–3). BoNTs and the structurally related tetanus neurotoxin (TeNT) constitute the clostridial neurotoxin (CNT) family. Although experimental evidence suggests that humans are sensitive to all CNTs, natural intoxications are associated only with TeNT and BoNT serotypes A, B, E, and F (1–4). In their active form, CNTs exist as dichain molecules linked by a single disulfide bond (3, 5, 6). CNTs are composed of an ~100-kDa heavy chain, which includes the toxin receptor-binding (HCR) and translocation domains, and an ~50-kDa light chain, which includes the protease domain. BoNT intoxication begins with the recognition of the neuronal presynaptic membrane. The HCR recognizes two co-receptor molecules (7); for serotypes that naturally intoxicate humans, these are a ganglioside and a protein (8–14). Upon receptor-mediated entry into the neuron and endosomal acidification, the heavy chain translocation domain facilitates translocation of the light chain into the host cell cytosol, where the disulfide bond is reduced and the light chain is released (15–18). The various light chains selectively cleave one or more neuronal SNARE (soluble *N*-ethylmaleimide attachment protein receptor) proteins (19–22). SNARE proteolysis destabilizes assembly of the SNARE core complex, abrogating synaptic vesicle exocytosis (23–26). The result of this proteolysis is that the innervated muscle or gland is paralyzed (27). Thus, BoNTs can, in theory, be used to treat a range of neurological conditions. TeNT intoxication is also initiated through recognition of co-receptor moieties on the presynaptic membrane of motor neurons. However, in contrast to the BoNTs, TeNT is rapidly sorted into the retrograde axonal pathway, leading to localized release of the toxin within the spinal cord. TeNT subsequently binds and enters adjacent inhibitory interneurons, where its catalytic activity is eventuated.

Early studies addressing CNT receptors present at nerve terminals quickly established a requirement for gangliosides (28–31). Despite these observations, the molecular basis of ganglioside recognition and the role that such molecules play in mediating toxin entry remain incomplete. BoNTs A, B, and F and TeNT all possess the conserved ganglioside-binding motif (GBM) (E/D) . . . H . . . SXWY . . . G. BoNT/E possesses a similar motif (E . . . K . . . SXWY . . . G), in which a lysine residue presumably replaces the conserved histidine (10, 32, 33). The GBM specifically associates with the GalNAc3-Gal4 moiety of the ganglioside neutral core region. Most notable, however, is that BoNTs bind only to gangliosides that have an α2,3-linked *N*-acetylneuraminic acid residue (denoted Sia5) attached to Gal4 of the oligosaccharide core (10, 33, 34), whereas the corresponding ganglioside-binding pocket on TeNT can also bind to GM1a, a ganglioside lacking the Sia5 sugar residue (supplemental Fig. S1) (32, 35). Together, these observations suggest that ganglioside-binding affinity and specificity are encoded by residues located outside of the conserved motif.

In this study, the crystal structure of the HCR of BoNT/F in complex with an oligosaccharide analog of ganglioside GD1a (GD1a-OS) is reported. Structure-based functional studies

* This work was supported, in whole or in part, by National Institutes of Health Grant U54 AI057153 from NIAID (to J.-J. P. K.) and Grant R00 NS061763 from NINDS (to M. R. B.). This work was also supported by grants from the Great Lakes Regional Center of Excellence.

[S] The on-line version of this article (available at http://www.jbc.org) contains supplemental Figs. S1 and S2 and Tables S1 and S2.

The atomic coordinates and structure factors (code 3RSJ) have been deposited in the Protein Data Bank, Research Collaboratory for Structural Bioinformatics, Rutgers University, New Brunswick, NJ (http://www.rcsb.org/).

[1] To whom correspondence should be addressed: Dept. of Molecular Microbiology and Immunology, University of Missouri, M618 Medical Sciences Bldg., Columbia, MO 65212. Fax: 573-882-4287; E-mail: baldwinmr@missouri.edu.

[2] The abbreviations used are: BoNT, botulinum neurotoxin; TeNT, tetanus neurotoxin; CNT, clostridial neurotoxin; HCR, heavy chain receptor-binding domain; GBM, ganglioside-binding motif; GD1a-OS, GD1a oligosaccharide.

were used to characterize the molecular properties of the interaction of BoNT/E/F and TeNT with gangliosides. These studies resulted in the development of a novel BoNT neurotoxin serotype F variant able to bind ganglioside in a manner independent of the Sia5 sugar residue. Additionally, these studies demonstrate that the conserved GBM is necessary but not sufficient for ganglioside binding and that additional residues, external to the GBM, are required to stabilize CNT-ganglioside interactions.

EXPERIMENTAL PROCEDURES

Reagents—Unless stated otherwise, molecular biology-grade chemicals and reagents were obtained from Sigma-Aldrich. *Escherichia coli* codon-optimized DNA constructs encoding HCR/A (residues 870–1295, YP_001253342), HCR/E (residues 843–1250, CAA43998), HCR/F (residues 862–1278, ADA79551), and HCR/T (residues 860–1310, AAK72964) were synthesized by EZBiolab (Westfield, IN). Vinyl 96-well plates (Corning Costar plate 2595) were obtained from Thermo Fisher Scientific.

HCR Expression and Purification—DNAs encoding CNT HCRs were subcloned into the pET-28 expression vector (Merck KGaA, Darmstadt, Germany). Mutant forms of HCR/E, HCR/F, and HCR/T were generated using the QuikChange II XL site-directed mutagenesis kit (Agilent) in accordance with the manufacturer's instructions. Purification of HCRs from *E. coli* BL21(DE3) was conducted as described previously (10) except that peak fractions from the Sephacryl S-200 HR column were concentrated using Amicon filtration devices (YM-50-type membrane). A typical purification from a 1-liter culture yielded between 5 and 25 mg of HCR depending on the serotype.

Trypsin Digests of Recombinant HCR Proteins—Briefly, recombinant HCR proteins (2 μg) were partially digested for 30 min at room temperature with trypsin (22.5 and 200 ng for HCR/F and HCR/E, respectively). SDS-PAGE loading dye was added to quench the digest, and the sample was loaded directly onto SDS-polyacrylamide gels. Proteins were visualized by staining with Coomassie Blue dye. Trypsin digestion did not reveal any differences in protein folding/stability (data not shown).

Crystallization, Data Collection, and Structure Solution and Refinement—Purified HCR/F was dialyzed against 20 mM Tris-HCl (pH 7.6) containing 500 mM NaCl and concentrated to a final concentration of 5 mg/ml. An oligosaccharide analog of ganglioside GD1a (GD1a-OS) was added to the concentrated HCR/F solution and incubated for several hours prior to the crystallization setup. Crystals were obtained by vapor diffusion using hanging drop techniques. Hanging drops containing 2 μl of 5 mg/ml HCR/F, 0.8 mM GD1a-OS, and 2 μl of well solution (100 mM HEPES (pH 7.0), 24% PEG 3350, and 200 mM $Mg(NO_3)_2$) were equilibrated against 0.5 ml of the well solution at 19 °C. The crystals of HCR/F complexed with the GD1a-OS belong to the triclinic space group P1, with cell dimensions a = 65.5, b = 84.3, and c = 117.6 Å and α = 72.6°, β = 67.1°, and γ = 84.1°. There are four molecules in an asymmetric unit with a Matthews coefficient of 2.8 $Å^3$/Da. The 2.4 Å data used in the initial molecular replacement were obtained at −175 °C using an in-house R-AXIS IV++ detector. HKL2000 (36) was used in the data processing. The 2.0 Å data used for the later stages of refinement were collected at Advanced Photon Source beamline SBC 19ID. Statistics for data collection and processing are summarized in Table 1.

The structure of the HCR/F·GD1a-OS complex was solved by the molecular replacement method with MOLREP within the CCP4 program suite (37) in the resolution range of 20–4.0 Å. The monomer structure of apo-HCR/F (Protein Data Bank code 3FUQ) was used as the search model. The initial structure obtained from molecular replacement was refined using the program CNS (38). The refinement protocol consisted of rigid body minimization, positional and temperature factor refinement, and simulated annealing. The coordinates of the GD1a-OS were obtained by modification of GT1b (Protein Data Bank code 1FV2). Sialic acid 7 of GT1b was deleted, and the β-form of sialic acid 6 was changed to the α-form. At this point, only part of the GD1a sugar moiety was visible in the $F_o - F_c$ difference map at the 2σ level. In one of the four molecules in the asymmetric unit, five sugar rings (Gal2(Sia6)-GalNAc3-Gal4-Sia5) can be fit into the density, four sugar rings can be fit into the second molecule (Gal2-GalNAc3-Gal4-Sia5), whereas only three sugar moieties (GalNAc3-Gal4-Sia5) can be found in the remaining two molecules. The structure was further refined with alternating manual adjustments using the TURBO-FRODO program package. The current model was completed with $R_{crystal}/R_{free}$ values of 0.232/0.263. The statistics of structural refinement are given in Table 1.

Ganglioside Binding Assay—Purified bovine brain gangliosides (GD1a or GM1a; Sigma) dissolved in methanol (1 mg/ml) were diluted in methanol and applied to non-protein-binding 96-well plates (5 μg of ganglioside/well). The solvent was evaporated at room temperature, and wells were washed with PBS and 0.04% (v/v) Tween 20. Nonspecific binding sites were blocked by incubation for 1 h in sodium carbonate buffer (pH 9.6) with 2% (w/v) BSA and 0.04% (v/v) Tween 20. Binding assays were performed in 100 μl of PBS with 0.04% (v/v) Tween 20 and 1% (w/v) BSA per well for 2 h at 4 °C and contained the designated HCR at the indicated concentrations. To control for potential effects caused by the proximity of the ligands to the plastic matrix, incomplete coating of substrates, etc., the appropriate wild-type HCR was used as an internal standard for each assay. Following incubation, plates were washed three times with PBS and 0.04% (v/v) Tween 20. An anti-FLAG monoclonal antibody M2 (1:8000; Sigma-Aldrich) and goat anti-mouse poly-HRP antibody (1:12,000; Pierce) mixture was added to wells for 20 min at 4 °C. Following incubation, plates were washed three times with PBS and 0.04% (v/v) Tween 20, and bound HCR was detected using Ultra TMB (Pierce) as the substrate for HRP. The reaction was terminated by the addition of 0.1 M H_2SO_4, and the absorbance at 450 nm was determined using an Epoch plate reader (BioTek).

Statistical Analysis—Half-maximal binding (B_{50}) was estimated by fitting ($R^2 > 0.90$) the data to the one-site binding equation ($Y = B_{max}\cdot X/(K_d + X)$) using GraphPad Prism. Data with $R^2 < 0.90$ were designated as $B_{50} > 10{,}000$ nM.

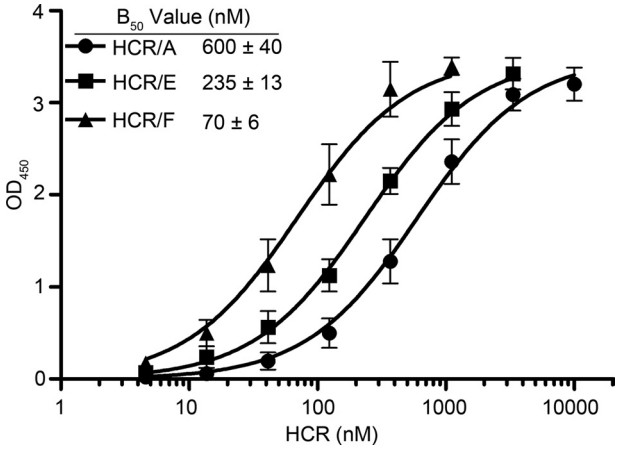

FIGURE 1. **Wild-type HCR binding kinetics.** Various concentrations of recombinant HCRs were examined for their ability to bind GD1a: HCR/A (●), HCR/E (■), and HCR/F (▲). B_{50} values represent half-maximal binding to the ganglioside. All values represent the arithmetic mean ± S.D. of at least four independent experiments performed in triplicate.

RESULTS

Properties of Binding of BoNT HCRs to GD1a—Although CNTs utilize gangliosides as co-receptor molecules for entry, our understanding of the mechanism(s) of ganglioside binding remains incomplete. Comparative analysis revealed that the HCRs of BoNTs A, E, and F display distinct affinities for binding to ganglioside GD1a, with HCR/F binding GD1a ~3-fold higher than HCR/E and 9-fold higher than HCR/A (Fig. 1). To better understand the mechanistic basis for these differences, we solved the crystal structure of HCR/F in complex with an analog of the GD1a-OS and conducted mutagenesis and binding studies to further characterize this interaction.

Structure of HCR/F in Complex with the GD1a-OS—The crystal structure of HCR/F in complex with an oligosaccharide analog of GD1a (GD1a-OS) was determined to a resolution of 2.0 Å by the molecular replacement method (Fig. 2*A* and Table 1). All of the monosaccharides in the GD1a analog were clearly defined by the electron density with the exception of glucose 1 (Fig. 2*B*). The structure of GD1a-OS-bound HCR/F is similar to the apo state (Protein Data Bank code 3FUQ), with an overall root mean square deviation of 0.5 Å (368 Cα atoms), with the notable exception of HCR/F residue Arg-1256, which undergoes a rotamer change upon binding. The GD1a-OS is bound at the distal tip of HCR/F, in a shallow groove formed by the side chains of His-1241 and Trp-1250, with Ser-1248 and Tyr-1251 forming the base of the pocket. The GalNAc3-Gal4 sugars of the GD1a-OS interact extensively with this site (Fig. 2*C*). The hydrophobic faces of both sugar rings are stacked against the indole ring of Trp-1250, whereas the polar faces are hydrogen-bonded to the protein (Fig. 2*C* and supplemental Table S1). Glu-1195 forms hydrogen bonds with both GalNAc3 and Gal4, whereas the side chains of His-1241 and Ser-1248 and the main chain carbonyl oxygens of Phe-1240 and His-1241 hydrogen bond to Gal4. Additional hydrogen bonds between HCR/F and Sia5 are formed by Arg-1111 and Arg-1256 and two bridging water molecules (Fig. 2*C* and supplemental Table S2).

Two Sia5-binding Arginine Residues Stabilize the HCR/F·GD1a-OS Complex—The importance of several residues in the binding of HCR/F to ganglioside GT1b has previously been identified by mutational studies (10). Mutations that lowered the affinity of HCR/F for GT1b were residues that make direct interactions with the GD1a carbohydrate moiety (Fig. 2*C*), which included Glu-1195, Ser-1248, and Trp-1250 (10). In addition, mutation of Tyr-1251 to Phe also reduced affinity for the ganglioside, an observation consistent with Tyr-1251 forming a hydrogen bond with Sia5 via a bridging water molecule (Fig. 2*C* and supplemental Table S2). However, the residues composing the conserved GBM cannot explain why binding of HCR/F to the ganglioside is dependent on the Sia5 sugar. The HCR/F·GD1a-OS complex identified two arginine residues (Arg-1111 and Arg-1256) that facilitate binding to the ganglioside through the formation of hydrogen bonds with Sia5 (Fig. 2*C*). These two arginine residues are not conserved among the BoNTs, suggesting there may be different mechanisms for ganglioside binding among the serotypes. Arg-1256 forms two hydrogen bonds with Sia5 (one direct and one via a bridging water molecule), and its mutation to alanine resulted in a 23-fold decrease in binding affinity, whereas mutation of Arg-1111 to alanine reduced the binding affinity by 8-fold (Fig. 3). By comparison, when both arginine residues were mutated, the binding affinity was 76-fold lower compared with the wild type, which is in agreement with our previous studies demonstrating the requirement of Sia5 for high affinity ganglioside binding (10).

HCR/F and HCR/E Bind GD1a by Distinct Mechanisms—BoNT/E is the most closely related CNT to BoNT/F, with a similarity score of 58.0% (ClustalW software) within the HCR. We therefore compared the HCR/F·GD1a-OS complex structure with the HCR derived from the previously solved structure of BoNT/E (Protein Data Bank code 3FFZ). Superposition analysis confirmed that the ganglioside-binding site of HCR/E is largely conserved, with Lys-1215 potentially fulfilling the role of His-1241 in HCR/F (Fig. 4). This was confirmed by mutation of Lys-1215 to histidine, resulting in a 19-fold decrease in binding affinity for GD1a; mutation to alanine abrogated binding (Fig. 5*A*). Another notable difference is the HCR/E loop located between α-helix 3 and β-strand 35 (residues 1228–1240), which has adopted a unique conformation relative to HCR/F. The Sia5-binding residues analogous to Arg-1111 and Arg-1256 in HCR/F are Lys-1093 and Arg-1230 in HCR/E (Fig. 4 and supplemental Fig. S2). However, mutation of Lys-1093 to alanine or arginine (the corresponding residue in HCR/F) had no effect on ganglioside binding. Similarly, mutation of Arg-1230 to alanine did not affect the ganglioside-binding activity of HCR/E (Table 2). Thus, the unique role of Arg-1111 and Arg-1256 in HCR/F receptor binding highlights a key difference in the mechanism of ganglioside recognition between the two serotypes.

Next, we investigated the effect of replacing histidine with lysine at the reciprocal position in HCR/F (H1241K). As shown in Fig. 5*B*, HCR/F^{H1241K} bound GD1a with 65-fold higher affinity than the wild type. We next investigated whether the loss of the interaction between Sia5 and Arg-1111 and Arg-1256 could be compensated for by the replacement of His-1241 with lysine. The triple-mutant protein HCR/$F^{R1111A,H1241K,R1256A}$ bound GD1a with a B_{50} value 17-fold greater than the double-mutant protein HCR/$F^{R1111A,R1256A}$ (Fig. 5*C*). These data demonstrate

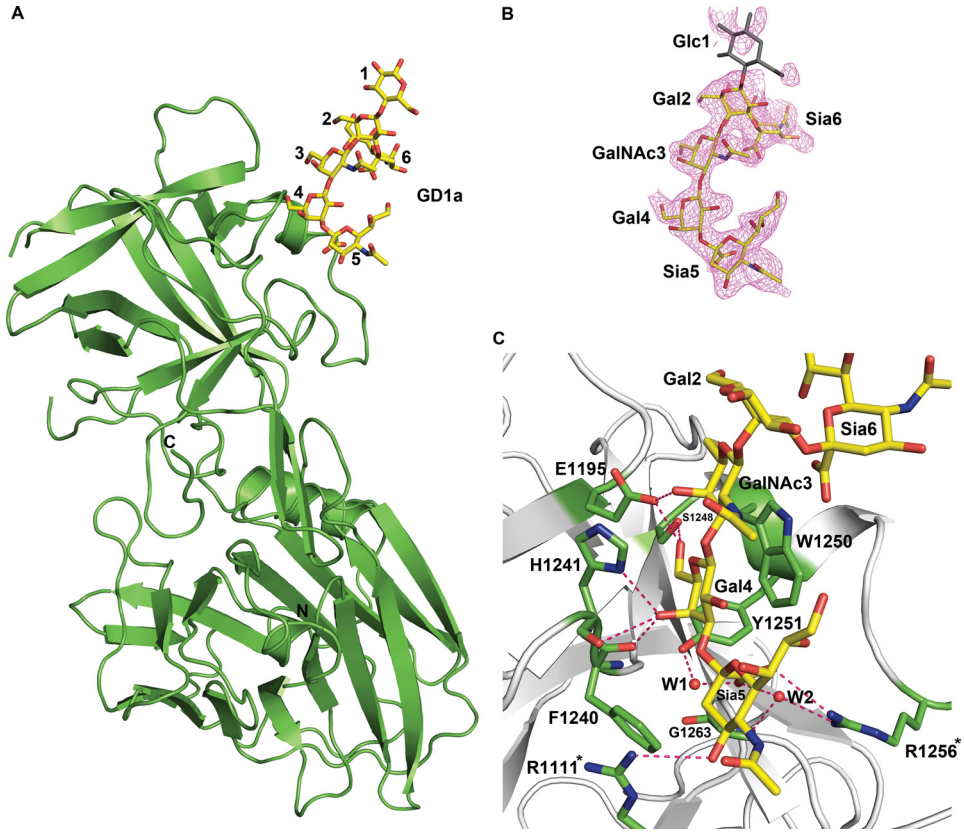

FIGURE 2. **Structure of HCR/F in complex with the GD1a-OS.** *A*, schematic representation of HCR/F shown in *green*. The GD1a-OS is shown as atomic color sticks. *B*, σ_A weighted $F_o - F_c$ omit map of the GD1a-OS contoured at 3.0σ. Electron density for glucose 1 (shown in *gray*) is not well defined. *C*, ribbon representation of the complex illustrating the positioning of the GD1a-OS in the ganglioside-binding cleft and the intermolecular hydrogen bond interactions. The two bridging water molecules are shown as *red spheres*. Residues not previously identified as contributing to ganglioside binding are highlighted *asterisks*.

TABLE 1
Data collection and refinement statistics (molecular replacement)

	HCR/F·GD1a
Data collection	
Space group	P1
Cell dimensions	a = 65.5, b = 84.3, c = 117.6 Å; α = 72.6°, β = 67.1°, γ = 84.1°
Resolution (Å)	30–2.0 (2.03–2.0)[a]
R_{sym}	0.059/0.409
I/σI	16.2 (2.1)
Completeness (%)	93.2 (65.5)
Redundancy	2.5 (2.2)
No. of molecules/asymmetric unit	4
Refinement	
Resolution (Å)	30–2.0
No. reflections	346,226
$R_{crystal}/R_{free}$	0.232/0.263
No. of atoms	
Protein	13,272
Ligand/ion	226
Water	424
B-factors(Å^2)	
Protein	41.1
Ligand/ion	70.0
Water	39.3
r.m.s.d.[b]	
Bond lengths (Å)	0.007
Bond angles	1.4°
Ramachandran plot (%)	
Most favored	82.7
Additionally allowed	16.5
Generously allowed	0.8
Disallowed	0.0

[a] Values in parentheses are for the highest resolution shell.
[b] r.m.s.d., root mean square deviation.

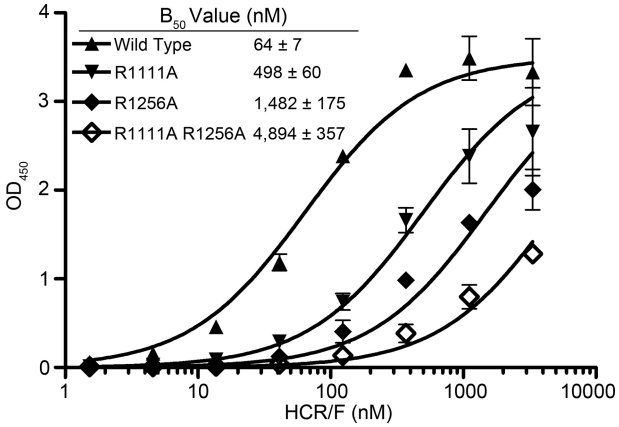

FIGURE 3. **Two arginine residues facilitate ganglioside binding at the Sia5 position.** Various concentrations of recombinant HCR/F proteins were examined for their ability to bind GD1a: wild type (▲), R1111A (▼), R1256A (◆), and R1111A,R1256A (◇). B_{50} values represent half-maximal binding to ganglioside. All values represent the arithmetic mean ± S.D. of two independent experiments performed in triplicate.

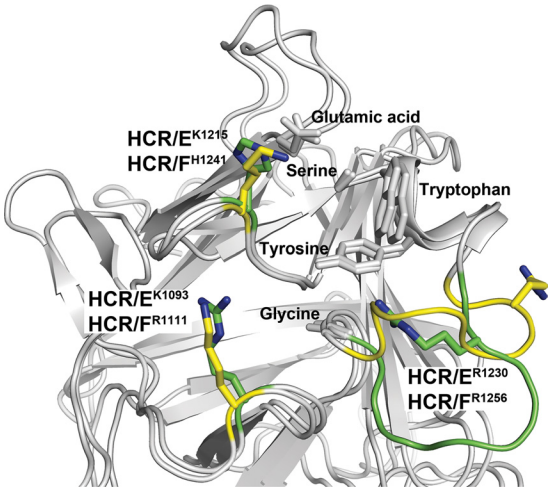

FIGURE 4. **Superposition of the HCR/E and HCR/F ganglioside-binding pockets.** Shown is a ribbon representation of HCR/F overlaid with the isolated HCR of BoNT/E (Protein Data Bank code 3FFZ). Residues constituting the conserved GBM of HCR/F and HCR/E are shown (stick representation). The key Arg-1111, His-1241, and Arg-1256 residues of HCR/F and the corresponding residues of HCR/E are highlighted (stick representation, atomic color). The altered loop region for HCR/F (Ile-1255–Asn-1262) is shown in *green*, and that for HCR/E (Met-1229–Asn-1236) is in *yellow*.

that the substitution of histidine with lysine in the consensus motif (E . . . H . . . SXWY . . . G) confers greater binding affinity (~20-fold) to the GalNAc3-Gal4 region of the ganglioside.

Unique Ganglioside Specificities of HCR/E and HCR/F^{H1241K}—On the basis of the observation that substitution of HCR/F His-1241 with lysine increased the affinity for the GalNAc3-Gal4 moiety of GD1a (Fig. 5, *B* and *C*), we reasoned that HCR/F^{H1241K} might bind the ganglioside with high affinity in a Sia5-independent manner. Consistent with our hypothesis, HCR/F^{H1241K} bound GM1a with a B_{50} value of 175 nM, whereas wild-type HCR/F had a B_{50} value beyond the limit of the assay (Fig. 5*D*). Although substitution of His-1241 with lysine conferred ganglioside binding to HCR/F in the absence of Sia5, wild-type HCR/E did not bind GM1a (Fig. 5*D*). This demonstrates that, similar to the other BoNT serotypes, HCR/E requires the presence of Sia5 to bind ganglioside. Furthermore, these observations highlight the unique ganglioside recognition strategies employed by BoNT serotypes E and F.

A Unique Asparagine Residue Stabilizes HCR/T^{R1226L}·Ganglioside Complexes—Numerous structural and biochemical studies have established that HCR/T contains two carbohydrate-binding sites: a lactose-binding site defined by the conserved GBM and a second sialic acid-binding site defined by a critical arginine residue (Arg-1226) (32, 35, 39). Therefore, to directly compare binding mediated through the conserved GBM, it is necessary to use a mutant form of the TeNT HCR (HCR/T^{R1226L}) in which the sialic acid-binding site is inactivated (32, 39). As shown in Fig. 6, HCR/T^{R1226L} bound to the ganglioside with a similar affinity as HCR/F. Previous structural and biochemical studies identified a unique asparagine residue within the lactose-binding site (Asn-1219) that interacts with ganglioside GT1b (32, 39, 40). To confirm the role of Asn-1219 in ganglioside binding, we screened the double-mutant HCR/T protein (HCR/T^{N1219A,R1226L}) in which both ganglioside-binding sites were mutated. Substitution of Asn-1219 with alanine abrogated binding to ganglioside GD1a (Fig. 6), consistent with the hypothesis that the GBM is necessary but not sufficient for ganglioside binding.

DISCUSSION

The binding of CNTs to nerve terminals is mediated through interactions with co-receptor moieties. Whereas TeNT displays high affinity for both a- and b-series gangliosides, BoNT serotypes associated with natural human intoxication (A, B, E, and F) preferentially bind to the terminal Gal4-Sia5 moiety of gangliosides GT1b and GD1a (supplemental Fig. S1) (10, 35, 39). Structural studies of HCR/A and HCR/T in complex with analogs of GT1b (Protein Data Bank codes 2VU9 and 1FV2, respectively) (40, 41) revealed that the ganglioside-binding pocket is largely defined by residues of the GBM ((E/D) . . . H . . . SXWY . . . G).

Here, we reported the crystal structure of the HCR of BoNT/F in complex with an analog of ganglioside GD1a (GD1a-OS). Similar to the BoNT/A·GT1b complex (41), the lack of structural changes upon GD1a-OS binding suggests that allosteric effects do not play a major role in the recognition of the SV2 protein co-receptor by HCR/F (10). HCR/F binds the GD1a-OS at the same binding site and in a similar manner to BoNT/A (Fig. 2) with a few noticeable differences. The carbonyl oxygen of HCR/F His-1241 is rotated toward the binding cleft and forms a hydrogen bond with Gal4, which is not present in BoNTs A, B, and E or TeNT. Another difference is in the coordination of the Sia5 moiety within GD1a, where Arg-1111 and Arg-1256 make bonds with Sia5 to stabilize ganglioside binding within the pocket (Figs. 2*C* and 3). Although dual substitution of both residues reduced affinity for GD1a (~76-fold) (Table 2), it did not ablate binding. In contrast, wild-type HCR/F did not bind GM1a, a ganglioside lacking Sia5 (Fig. 5*D*) (10) . We therefore propose that binding of HCR/F to Sia5 is additionally stabilized through hydrophobic interactions of the Sia5 ring with the side chains of Leu-1110 and Phe-1240 and the aliphatic moiety of Arg-1111. The presence of hydrophobic groups at the corresponding positions in BoNTs A and E suggests that this may be a conserved interaction shared among a subset of the

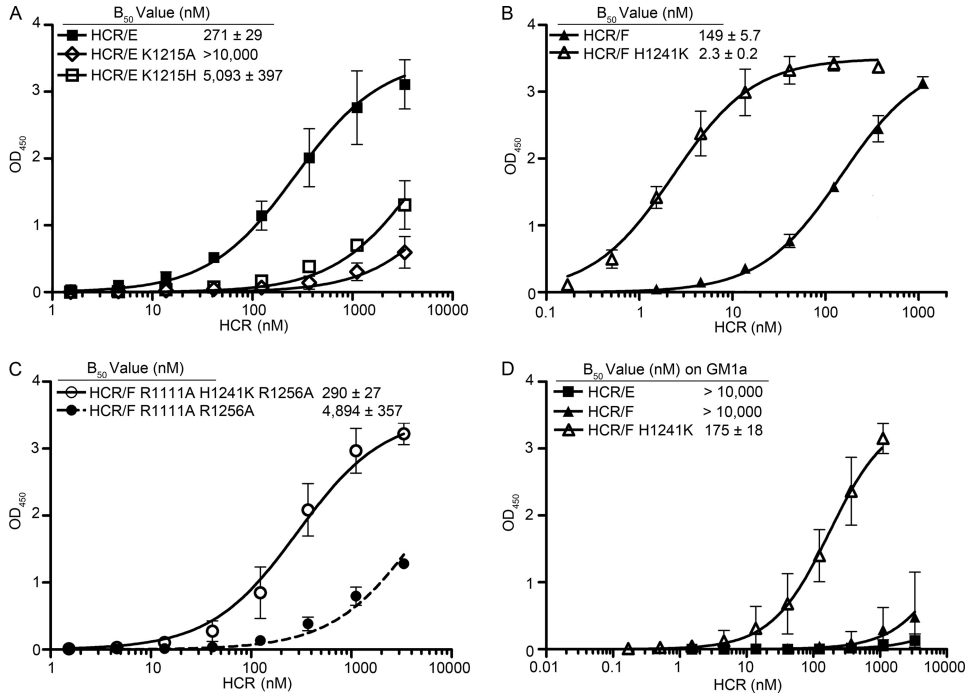

FIGURE 5. **Comparative analysis of HCR binding to gangliosides GD1a and GM1a.** Various concentrations of the recombinant HCRs were examined for their ability to bind GD1a. *A*, HCR/E (■), HCR/E^{K1215A} (◇), and HCR/E^{K1215H} (□). *B*, HCR/F (▲) and HCR/F^{H1241K} (△). *C*, HCR/$F^{R1111A,H1241K,R1256A}$ (○) and HCR/$F^{R1111A,R1256A}$ (●; compared using data from Fig. 3). *D*, various concentrations of recombinant HCR/E (■), HCR/F (▲), and HCR/F^{H1241K} (△) were examined for their ability to bind GM1a. B_{50} values represent half-maximal binding to ganglioside. Values represent the arithmetic mean ± S.D. of three independent experiments performed in triplicate.

TABLE 2

HCR variant -fold change in ganglioside binding compared with wild-type HCR

Protein	Relative affinity[a]
HCR/F^{R1111A}	0.13
HCR/F^{R1256A}	0.04
HCR/$F^{R1111A,R1256A}$	0.01
HCR/F^{H1241K}	65
HCR/$F^{R1111A,H1241K,R1256A}$	0.25
HCR/E^{K1093A}	4
HCR/E^{K1093R}	1
HCR/E^{K1215A}	
HCR/E^{K1215H}	0.05
HCR/E^{R1230A}	0.59

[a] Values standardized to the wild-type control for each data set.

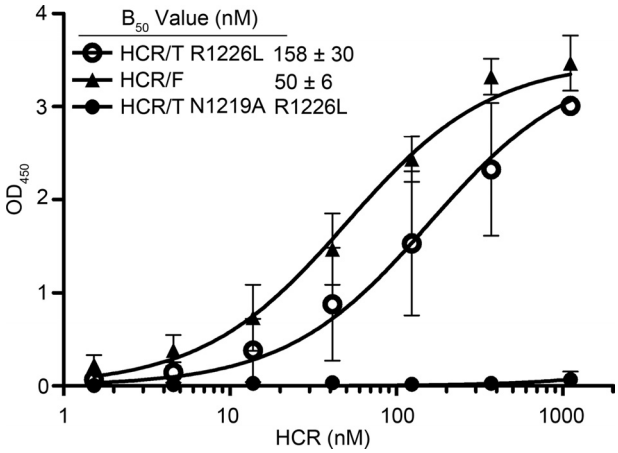

FIGURE 6. **Mutational analysis of the lactose-binding site in the tetanus receptor-binding domain (HCR/T).** The lactose-binding binding site in HCR/T is structurally similar to the ganglioside-binding site in the botulinum HCRs. Various concentrations of the recombinant wild-type and variant HCRs for HCR/T^{R1226L} (○), HCR/F (▲), and HCR/$T^{N1219A,R1226L}$ (●) were examined for their ability to bind GD1a. B_{50} values represent half-maximal binding to ganglioside. All values represent the arithmetic mean ± S.D. of two independent experiments performed in triplicate.

BoNTs. In TeNT (which does not require Sia5 for ganglioside binding), the comparable residues are Ala-1134, Ser-1135, and Thr-1270, and thus, hydrophobic interactions are largely absent.

The ganglioside-binding pockets of BoNTs A, B, and F and TeNT are all characterized by the presence of the consensus GBM ((E/D) . . . H . . . SXWY . . . G). Although residues within the GBM are necessary for interaction with the GalNAc3-Gal4 moiety, the GBM is not sufficient to facilitate ganglioside binding. Thus, additional residues are required to stabilize the interaction between the toxin and the ganglioside (summarized in Fig. 7). In the case of HCR/A, Tyr-1117 and Ser-1275 form hydrogen bonds with Sia5, which, in conjunction with additional hydrophobic interactions between the HCR and Sia5, act to stabilize ganglioside binding (41). Although Tyr-1117 and Ser-1275 of HCR/A are not conserved among the BoNTs, our studies have revealed that Arg-1111 and Arg-1256 perform an analogous function in HCR/F (Figs. 2*C* and 7). We therefore propose that binding of Sia5 through residues located outside of the GBM is a mechanism shared by BoNTs A and F. Structural and biochemical studies of TeNT confirmed that ganglioside binding is not dependent on Sia5, as is the case for BoNTs A, B, E, and F (39, 40). Rather, TeNT stabilizes its binding to gangliosides through a unique asparagine residue (Asn-1219) that hydrogen bonds to GalNAc3 (Figs. 6 and 7) (32, 40). Mutation of Asn-1219 abrogated binding to GD1a (this study) and severely attenuated cellular toxicity, consistent with the con-

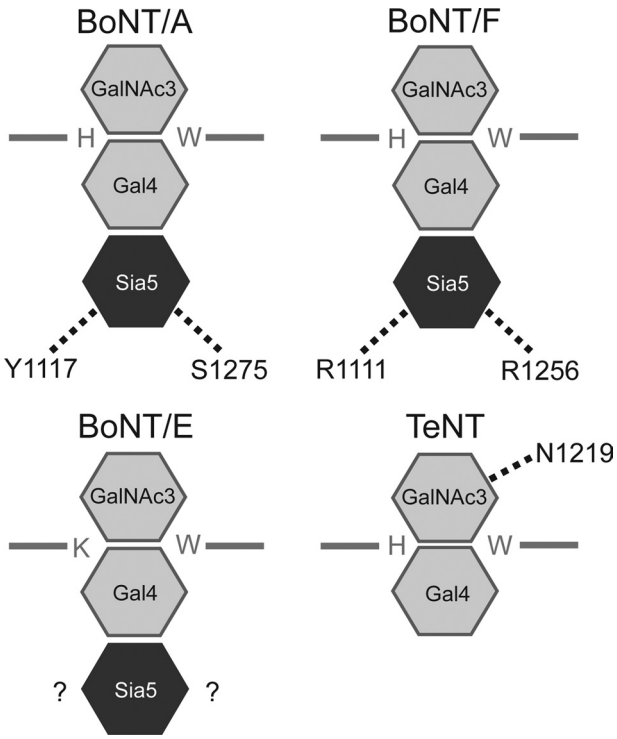

FIGURE 7. **Schematic of HCR-mediated ganglioside binding.** In each of the panels, monosaccharides are represented by *hexagons*. GalNAc3 and Gal4 are colored in *light gray*, whereas Sia5 is colored in *dark gray*. HCR amino acid residues involved in ganglioside binding are represented using their single-letter codes. Hydrogen bonds are indicated by *dotted lines* between the amino acid in question and the indicated sugar.

cept that the GBM alone is insufficient to mediate ganglioside binding (32). Therefore, Asn-1219 fulfills a function in TeNT analogous to the role of residues that hydrogen bond to Sia5 in the BoNTs. However, the interaction of Asn-1219 with GalNAc3, rather than Sia5, confers upon TeNT the unique ability to bind gangliosides such as GM1a (supplemental Fig. S1).

Although the overall architecture of the BoNT/E ganglioside-binding pocket is conserved among the CNTs, the conserved GBM is not present. Rather, BoNT/E possesses a similar motif (E . . . K . . . SXWY . . . G) in which a lysine residue replaces the conserved histidine. Studies of both wild-type and mutant forms of HCR/E and HCR/F (Fig. 5, *A* and *B*) demonstrated that substitution of histidine with lysine within the GBM increased affinity for the GalNAc3-Gal4 moiety by ~20-fold. At present, the mechanism by which replacement of histidine with lysine changes affinity for the ganglioside remains unclear. Molecular modeling studies suggest that the lysine side chain can potentially form two additional hydrogen bonds with the GD1a-OS relative to histidine (data not shown), which could account for the increased affinity for GD1a. Studies to co-crystallize the HCR/F^{H1241K} protein with GD1a-OS are currently under way.

In addition to increasing affinity for GD1a, replacement of HCR/F His-1241 with lysine was sufficient to alleviate the dependence of HCR/F on the Sia5 sugar, conferring the ability to bind ganglioside GM1a (Fig. 5*D*). This observation is consistent with our model that residues forming the conserved GBM are necessary but not sufficient to mediate ganglioside binding (Fig. 7). To our knowledge, this is the first demonstration of a mutation resulting in an altered ganglioside-binding specificity.

Given these observations, we anticipated that HCR/E would bind gangliosides in a manner reminiscent of the HCR/F^{H1241K} protein. However, binding of HCR/E to ganglioside GM1a was not detectable under our assay conditions. This raised the obvious question of why HCR/E is dependent on Sia5 for ganglioside binding. Superposition analysis of HCR/E (Protein Data Bank code 3FFZ) revealed a major difference in conformation of the loop region (residues 1228–1240) linking the conserved tyrosine and glycine of the GBM (Fig. 4). However, the introduction of this loop into the corresponding region of HCR/F^{H1241K} did not prevent binding of the protein to GM1a (data not shown). This suggests that the conformation of this loop region is not the major determinant of ganglioside-binding specificity. This is further supported by our observation that HCR/E Arg-1230 does not fulfill a role analogous to the corresponding residue in HCR/F (Arg-1256) (Table 2). Ongoing studies to co-crystallize HCR/E with the GD1a-OS will likely explain the dependence of HCR/E on Sia5 for ganglioside binding.

Preliminary experiments suggest that binding and entry of HCR/F^{H1241K} into cultured neurons occur via the same mechanism as for the wild-type protein, albeit at significantly lower concentrations (data not shown). Replacement of histidine with lysine did not alter the sensitivity of binding to pH, as both the wild-type and mutant proteins bound GD1a with similar affinities under conditions ranging from pH 4.5 to 7.5 (data not shown). This observation suggests that BoNT/F remains bound to the ganglioside under conditions encountered within the endosome. Moreover, the increased ganglioside-binding affinity of HCR/F^{H1241K} is unlikely to affect light chain translocation. Presumably, the increased binding and entry of HCR/F^{H1241K} into cultured neurons will translate into increased toxicity of the BoNT/F^{H1241K} holotoxin. If developed as a pharmacologic agent, this engineered form of BoNT may enhance the treatment of neurological disorders. In conclusion, this study has demonstrated that residues located outside of the conserved GBM contribute to both ganglioside-binding affinity and specificity and may assist in explaining the differing pathological manifestations of the CNTs.

Acknowledgments—The GD1a analog (compound Te303) utilized in this study was provided by Consortium for Functional Glycomics Grant GM62116. We thank the staff at Advanced Photon Source beamline SBC 19ID for excellent assistance in data collection and Dr. Joseph T. Barbieri for helpful suggestions during the preparation of this manuscript.

REFERENCES

1. Arnon, S. S., Schechter, R., Inglesby, T. V., Henderson, D. A., Bartlett, J. G., Ascher, M. S., Eitzen, E., Fine, A. D., Hauer, J., Layton, M., Lillibridge, S., Osterholm, M. T., O'Toole, T., Parker, G., Perl, T. M., Russell, P. K., Swerdlow, D. L., and Tonat, K. (2001) *JAMA* **285,** 1059–1070
2. Johnson, E. A. (1999) *Annu. Rev. Microbiol.* **53,** 551–575
3. Johnson, E. A., and Bradshaw, M. (2001) *Toxicon* **39,** 1703–1722
4. Hatheway, C. L. (1995) *Curr. Top. Microbiol. Immunol.* **195,** 55–75
5. Baldwin, M. R., Kim, J. J., and Barbieri, J. T. (2007) *Nat. Struct. Mol. Bio.l* **14,** 9–10

6. Lacy, D. B., Tepp, W., Cohen, A. C., DasGupta, B. R., and Stevens, R. C. (1998) *Nat. Struct. Biol.* **5,** 898–902
7. Montecucco, C., Rossetto, O., and Schiavo, G. (2004) *Trends Microbiol.* **12,** 442–446
8. Dong, M., Liu, H., Tepp, W. H., Johnson, E. A., Janz, R., and Chapman, E. R. (2008) *Mol. Biol. Cell* **19,** 5226–5237
9. Dong, M., Yeh, F., Tepp, W. H., Dean, C., Johnson, E. A., Janz, R., and Chapman, E. R. (2006) *Science* **312,** 592–596
10. Fu, Z., Chen, C., Barbieri, J. T., Kim, J. J., and Baldwin, M. R. (2009) *Biochemistry* **48,** 5631–5641
11. Kitamura, M., Iwamori, M., and Nagai, Y. (1980) *Biochim. Biophys. Acta* **628,** 328–335
12. Nishiki, T., Tokuyama, Y., Kamata, Y., Nemoto, Y., Yoshida, A., Sato, K., Sekiguchi, M., Takahashi, M., and Kozaki, S. (1996) *FEBS Lett.* **378,** 253–257
13. Ochanda, J. O., Syuto, B., Ohishi, I., Naiki, M., and Kubo, S. (1986) *J. Biochem.* **100,** 27–33
14. Yeh, F. L., Dong, M., Yao, J., Tepp, W. H., Lin, G., Johnson, E. A., and Chapman, E. R. (2010) *PLoS Pathog.* **6,** e1001207
15. Fischer, A., and Montal, M. (2007) *J. Biol. Chem.* **282,** 29604–29611
16. Koriazova, L. K., and Montal, M. (2003) *Nat. Struct. Biol.* **10,** 13–18
17. Montecucco, C., Schiavo, G., and Dasgupta, B. R. (1989) *Biochem. J.* **259,** 47–53
18. Simpson, L. I. (1989) *J. Pharmacol. Exp. Ther.* **251,** 1223–1228
19. Blasi, J., Chapman, E. R., Link, E., Binz, T., Yamasaki, S., De Camilli, P., Südhof, T. C., Niemann, H., and Jahn, R. (1993) *Nature* **365,** 160–163
20. Schiavo, G., Benfenati, F., Poulain, B., Rossetto, O., Polverino de Laureto, P., DasGupta, B. R., and Montecucco, C. (1992) *Nature* **359,** 832–835
21. Schiavo, G., Santucci, A., Dasgupta, B. R., Mehta, P. P., Jontes, J., Benfenati, F., Wilson, M. C., and Montecucco, C. (1993) *FEBS Lett.* **335,** 99–103
22. Schiavo, G., Shone, C. C., Rossetto, O., Alexander, F. C., and Montecucco, C. (1993) *J. Biol. Chem.* **268,** 11516–11519
23. Jahn, R., and Grubmüller, H. (2002) *Curr. Opin. Cell Biol.* **14,** 488–495
24. Weber, T., Zemelman, B. V., McNew, J. A., Westermann, B., Gmachl, M., Parlati, F., Söllner, T. H., and Rothman, J. E. (1998) *Cell* **92,** 759–772
25. Sutton, R. B., Fasshauer, D., Jahn, R., and Brunger, A. T. (1998) *Nature* **395,** 347–353
26. Jahn, R., and Scheller, R. H. (2006) *Nat. Rev. Mol. Cell Biol.* **7,** 631–643
27. Davletov, B., Bajohrs, M., and Binz, T. (2005) *Trends Neurosci.* **28,** 446–452
28. Van Heyningen, W. E. (1961) *Br. J. Exp. Pathol.* **42,** 397–398
29. Van Heyningen, W. E., and Miller, P. A. (1961) *J. Gen. Microbiol.* **24,** 107–119
30. Simpson, L. L., and Rapport, M. M. (1971) *J. Neurochem.* **18,** 1761–1767
31. Simpson, L. L., and Rapport, M. M. (1971) *J. Neurochem.* **18,** 1341–1343
32. Rummel, A., Bade, S., Alves, J., Bigalke, H., and Binz, T. (2003) *J. Mol. Biol.* **326,** 835–847
33. Rummel, A., Mahrhold, S., Bigalke, H., and Binz, T. (2004) *Mol. Microbiol.* **51,** 631–643
34. Rummel, A., Häfner, K., Mahrhold, S., Darashchonak, N., Holt, M., Jahn, R., Beermann, S., Karnath, T., Bigalke, H., and Binz, T. (2009) *J. Neurochem.* **110,** 1942–1954
35. Chen, C., Fu, Z., Kim, J. J., Barbieri, J. T., and Baldwin, M. R. (2009) *J. Biol. Chem.* **284,** 26569–26577
36. Minor, W., Tomchick, D., and Otwinowski, Z. (2000) *Structure* **8,** R105–R110
37. Dodson, E. J., Winn, M., and Ralph, A. (1997) *Methods Enzymol.* **277,** 620–633
38. Brunger, A. T. (2007) *Nat. Protoc.* **2,** 2728–2733
39. Chen, C., Baldwin, M. R., and Barbieri, J. T. (2008) *Biochemistry* **47,** 7179–7186
40. Fotinou, C., Emsley, P., Black, I., Ando, H., Ishida, H., Kiso, M., Sinha, K. A., Fairweather, N. F., and Isaacs, N. W. (2001) *J. Biol. Chem.* **276,** 32274–32281
41. Stenmark, P., Dupuy, J., Imamura, A., Kiso, M., and Stevens, R. C. (2008) *PLoS Pathog.* **4,** e1000129